

## Synthesis of $\text{Na}_3\text{Fe}_2(\text{PO}_4)_3$ with NASICON-Type Structure from Ferrous Oxalate Precursor in the Presence of Colloidal Silicon Dioxide

Lubomir Teoharov<sup>1</sup>, Plamen Penev<sup>2\*</sup>, Meelis Härmas<sup>3</sup> and Alar Jänes<sup>3</sup>

<sup>1</sup>Bultechnoplus- Ltd, Sofia, Bulgaria

<sup>2</sup>Simlogic- Ltd, Sofia, Bulgaria

<sup>3</sup>Institute of Chemistry, University of Tartu, Tartu, Estonia

### ABSTRACT

The widespread presence of sodium in the earth's crust, the significant stability of its compounds and its great ecological recycling possibilities are all factors that lead researchers to new structures exhibiting ion migration of sodium and high electrochemical potential. The present research shows a new way for  $\text{Na}_3\text{Fe}_2(\text{PO}_4)_3$  synthesis with Na Super Ion Conductor structure. The use of ferrous oxalate precursor  $\text{Na}_3\text{Fe}(\text{C}_2\text{O}_4)_3$  changes the reaction pathway of the iron-phosphate system synthesis and leads to the formation of a structure that allows ion migration that enhances electrochemical charge storage properties. At best the measured capacity was 85 mAh g<sup>-1</sup> over a voltage range of 4.2 V to 1.5 V vs Na/Na<sup>+</sup>. It is shown that the presence of colloidal silicon dioxide helps the main phase crystallization, without entering its structure.

### Corresponding authors

Plamen Penev, SimLogic – Ltd, Tzvetan Lazarov Bld.33 office 8, 1592-Sofia, Bulgaria.

**Received:** February 20, 2023; **Accepted:** February 22, 2023; **Published:** February 28, 2023

**Keywords:** Ferrous Oxalate Precursor, Silicon Dioxide,  $\text{Na}_3\text{Fe}_2(\text{PO}_4)_3$ , NASICON-Type Structure

### Introduction

Lithium-ion batteries are regarded as the state-of-the-art technology for energy storage and conversion. However, the resources of lithium on the earth are limited and the price of lithium increased significantly over the past years. Therefore, the lithium-ion battery is not a wise choice for large-scale energy storage [1]. Sodium has many advantages as a material in batteries, especially in cost, which is the key factor for large-scale stationary energy storage. Sodium is the 4th most abundant element in the earth's crust with near-infinite resources in principle. Sodium-ion batteries therefore meet the need for a low-cost system if the other components are also sustainable that can integrate discontinuous renewable energy sources and optimize the performance of electricity grids [2-4].

The crystal structure of the prototype NASICON (a term for “Na Super Ion Conductor”) compound  $\text{NaZr}_2(\text{PO}_4)_3$  was first reported by Hagman et al., but it was in 1976 when the structure type attracted wide attention after Goodenough and Hong demonstrated very high Na<sup>+</sup>-ion conductivity in  $\text{Na}_{1-x}\text{Zr}_2\text{Si}_x\text{P}_{3-x}\text{O}_{12}$  [5-7].

As is known, hard electrolytic materials can be grouped in three main fields: anion conductors with fluorite structure, cation conductors with  $\beta$ - and  $\beta'$ - $\text{Al}_2\text{O}_3$  structures, and cation conductors with NASICON structure, the ion transport number of which is well established to be  $\geq 0.99$  [8].

Research on  $\text{Na}_3\text{Fe}_2(\text{PO}_4)_3$  shows this compound belongs to a monoclinic crystal system with crystal lattice parameters ( $a = 15.070 \text{ \AA}$ ,  $b = 8.740 \text{ \AA}$ ,  $c = 8.724 \text{ \AA}$ ,  $\alpha = \gamma = 90.0^\circ$  and  $\beta = 125.1^\circ$ ), while the crystal structure consists of  $\text{FeO}_6$ -octahedrons and  $\text{PO}_4$ -tetrahedrons with shared corners [9]. That sharing of corners between the octahedrons and the tetrahedrons forms cavities via which the transport of sodium ions through the structure is conducted. For this reason the ion conductivity sets structural requirements for the methods of synthesis, the composition and the conditions under which the material is treated.

Anantharamulu et al. produce a thorough survey of the possible component options when synthesizing NASICON of the  $\text{AM}_1\text{M}_2(\text{PO}_4)_3$  type, where “A” may be an alkaline ion (Li, Na, K, Rb,  $\text{NH}_4$ ), an alkaline earth ion (Mg, Ca, Sr, Ba), “M<sub>1</sub>” and “M<sub>2</sub>” can be of the bivalent ion group (Zn, Cd, Ni, Co), trivalent ions of Fe, V, Al, Ti or ions of Zr, Hf, Si, As with higher valence [10].

Carlier et al. reported  $\text{Na}_3\text{Fe}_3(\text{PO}_4)_4$  as the cathode material in sodium ion batteries; however, the electrochemical performance of the layered  $\text{Na}_3\text{Fe}_3(\text{PO}_4)_4$  compound was not attractive. As we know, iron-based phosphate compounds have rich and complex structural chemistry [11-12]. The multiplicity of variants in terms of composition of the materials also suggests different ways of synthesis. It is our opinion that the traditional means of synthesis such as solid-phase and the sol-gel process or their variants are limited in a technological sense when creating materials with preliminarily given properties and controlled stages of multi-

component interaction. Such capabilities are offered by the so-called “water methods” or synthesis in a water environment with precise physicochemical control of the reaction pathways.

In this research we present a method for the synthesis of NASICON type  $\text{Na}_3\text{Fe}_2(\text{PO}_4)_3$  by oxalate precursor in a water environment. The electrochemical activity results of the material bear a typical ion-conducting system signature.

### Description of the Experiment

The  $\text{Na}_3\text{Fe}_2(\text{PO}_4)_3$  synthesis of NASICON type by the given method is an original work, described in a patent application [13]. A chemical environment in the synthesis is created by a precursor of iron, which has a leading chemical role, namely: sodium ferrioxalate -  $\text{Na}_3\text{Fe}(\text{C}_2\text{O}_4)_3$ . The other main reagent is the phosphate precursor  $\text{NaH}_2(\text{PO}_4)$ . The oxalate precursor's role is to change the chemical interaction between the iron and  $\text{NaH}_2(\text{PO}_4)_3$ , thus creating conditions for another reaction pathway in  $\text{Na}_3\text{Fe}_2(\text{PO}_4)_3$  synthesis. Second, a promoting component is introduced in the reaction environment (alkaline stabilized colloidal solution of  $\text{SiO}_2$  - silicazol), which helps crystallization of the target product, without entering its chemical and crystallographic structure in the synthesis conditions described. The invented method is founded on the very well expressed property of the oxalate ion to form complex compounds with many metals, particularly iron, forming the compound  $\text{Na}_3\text{Fe}(\text{C}_2\text{O}_4)_3$ . It is known that this complex structure is also preserved in a solution [14]. Iron is bonded with the dibasic oxalate ion via oxygen bridges that stabilize it, thus the ion has a specific behavior in acid-neutralization reactions that differs from the behavior of iron in its other compounds (chlorides, sulfates and nitrates). If hydrolysis and formation of ferric hydroxide complexes are characteristic of ferrous compounds during the neutralization process as soon as  $pH$  is around 3, in the case of the ferrioxalate ion these interactions become noticeable only at neutral  $pH$ . Obtaining ferric hydrate complex by oxalate precursor that leads to iron hydroxide with ferrihydrite structure only at  $pH$  above 7 in the presence of hydrolyzing alkaline reagent is proven in an earlier research [15].

The chemical interaction of the two precursors in the presence of hydrolyzing agent  $\text{NaOH}$  is described by Equation (1):



The iron phosphate  $\text{FePO}_4$  is a compound with very low solubility and when in the presence of phosphoric acid salts (acidic or normal phosphates) in a solution of iron salts of mineral acids (nitrates, sulfates or chlorides), it precipitates as the most energetically preferred chemical structure as soon as  $pH$  is around 3, existing as a stable amorphous structure that crystallizes when thermally influenced above  $550^\circ\text{C}$ . When oxalate environment is present, however, the formation of  $\text{FePO}_4$  takes place in the neutral  $pH$  region of around 7.

Figure 1 presents the thermal behavior of the obtained precipitate, which keeps its amorphous structure even at thermal influence of up to  $600^\circ\text{C}$ , which proves the strong influence of the oxalate environment.

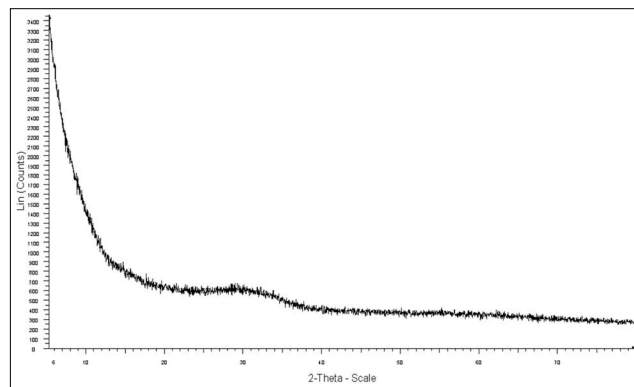


Figure 1: XRD of the precipitate after firing at  $600^\circ\text{C}$  - 1 hour

### Experiments and Results

The  $\text{Na}_3\text{Fe}_2(\text{PO}_4)_3$  synthesis begins with dissolving 7.77 g (0.02 mol)  $\text{Na}_3\text{Fe}(\text{C}_2\text{O}_4)_3$  in 100 ml distilled water and the preparation of a solution of 3.28 g (0.02 mol)  $\text{NaH}_2\text{PO}_4$  and 2.4 g (0.06 mol)  $\text{NaOH}$  in 50 ml distilled water at around  $45^\circ\text{C}$  until dissolved. Separately, 7.56 g (0.06 mol)  $\text{H}_2\text{C}_2\text{O}_4$  is dissolved in 100 ml water, after which 2-4 ml of alkaline stabilized 40 % silicazol solution (0.014 mol  $\text{SiO}_2$ ) is added in the oxalate solution. The second solution, containing the phosphate precursor, is mixed with the oxalate solution that contains silicazol and the solution of  $\text{Na}_3\text{Fe}(\text{C}_2\text{O}_4)_3$  is added to both all at once, while stirring until reaching homogenization and clarity. The solution thus obtained not only contains equivalent amount of the precipitator  $\text{Na}_3\text{PO}_4$ , but also contains three times the molar excess of oxalate ions, calculated in relation to the amount of  $\text{Na}_3\text{Fe}(\text{C}_2\text{O}_4)_3$ . It is stirred while heated to  $35^\circ\text{C}$  for a time of 30 min and when first indications of gelling appear 10 % of  $\text{NaOH}$  solution is slowly added until  $pH$  reaches 7–7.5, which leads to a jelly-like deposit. Stirring continues for 15 min more and then it is filtered by washing the deposit on top of the filter until there are no more oxalate ions in the filter (controlled by the permanganate method). After drying at  $140^\circ\text{C}$  the deposit is baked at  $600^\circ\text{C}$  for 2 h and is characterized by means of X-ray diffraction (XRD). The observed X-ray diagram explicitly proves crystal phase  $\text{Na}_3\text{Fe}_2(\text{PO}_4)_3$ , as seen in Figure 2. The material thusly obtained is called NASICON 1. Through the same procedure, but without the presence of colloidal silicon dioxide, a material is synthesized called NASICON 2. As is seen, the presence of colloidal silicon dioxide does not lead to the formation of other crystal phases, neither is it included in the forming  $\text{Na}_3\text{Fe}_2(\text{PO}_4)_3$  structure at thermal treatment at  $600^\circ\text{C}$ . XRD patterns of the formed NASICON-type structures are practically the same, which shows that the influence of the  $\text{SiO}_2$  on the electrochemical activity of the material has a different nature and is not connected to the crystallographic structure of the active phase.

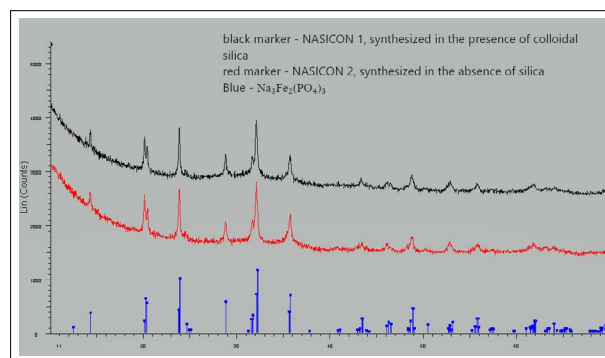
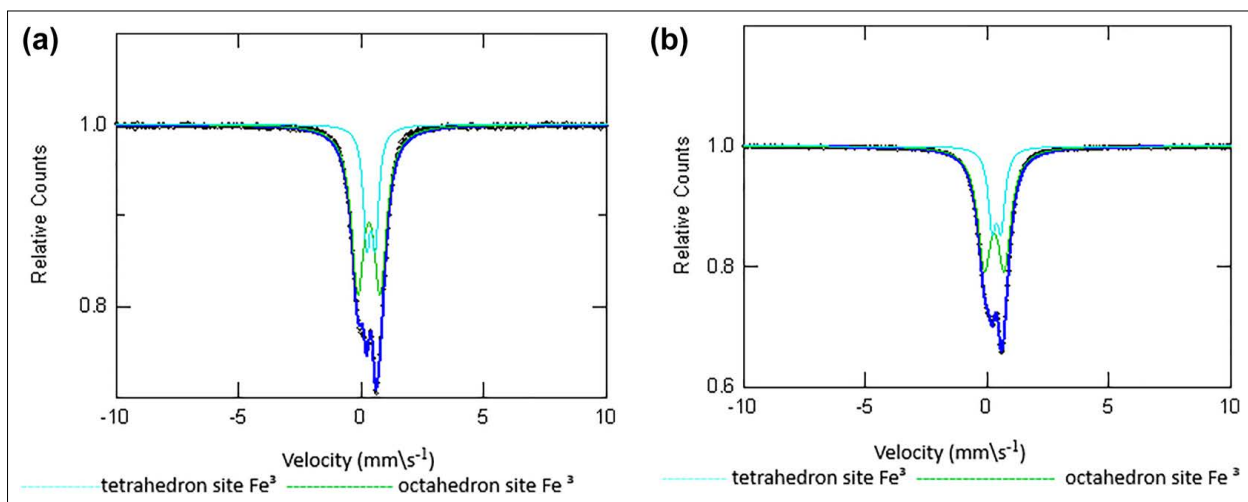


Figure 2: XRD after drying at  $140^\circ\text{C}$ ; the deposit is baked at  $600^\circ\text{C}$  for 2 h in the presence of silica (a), without the presence of silica (b).

The samples, obtained after heating, are examined via Mössbauer spectroscopy and are named NASICON 1 and NASICON 2, respectively (Table 1). The result is presented in Figure 3. Research was conducted using an electromechanical spectrometer (Wissenschaftliche Elektronik GMBN, Germany) in a constant acceleration mode at room temperature. The source used was  $^{57}\text{Co}/\text{Rh}$  (Activity@15 mCi), standard -  $^*\text{-Fe}$ . The experimentally obtained spectrum is processed with the WINNORMOS program. The experimental spectrum of NASICON 2 (a sample without  $\text{SiO}_2$ ) is comprised of two doublets. The calculated parameters of doublet component Db1, which has relatively low mass 28 %, correspond to  $\text{Fe}^{3+}$  in the structure of  $\text{Na}_3\text{Fe}_2(\text{PO}_4)_3$  [16]. The doublet with larger quadrupole splitting (Db2) can be attributed to  $\text{Fe}^{3+}$  in Na-Fe-phosphate glass [17]. The differentiated values of the quadrupole separation Db1 and Db2 are typical for  $\text{Na}_3\text{Fe}_2(\text{PO}_4)_3$  and iron-phosphate glasses. The blue curve shows the doublet of the tetrahedral configuration of  $\text{Fe}^{3+}$  in the quadrupole separation Db1 value characteristic for  $\text{Na}_3\text{Fe}_2(\text{PO}_4)_3$ , and the curve of the second doublet in green shows the octahedral configuration of  $\text{Fe}^{3+}$  in phosphate glasses with quadrupole separation Db2. Their clear differentiation indicates that at a temperature of 600 °C the two phases exist independently without being incorporated in partial or mutual structure. This examination shows that the  $\text{SiO}_2$  introduced during the synthesis of  $\text{Na}_3\text{Fe}_2(\text{PO}_4)_3$  does not change the surrounding environment of the iron atom and does not enter into the structure of the synthesized compound, and the vitreous phase is phosphate glass existing as a separate amorphous structure without the involvement of silicon dioxide at the temperature of the synthesis (600 °C).

**Table 1: The NASICON samples examined via Mössbauer spectroscopy**

Sample	Components	$\delta$ ( $\text{mm s}^{-1}$ )	$\Delta$ ( $\text{mms}^{-1}$ )	$\Gamma$ exp ( $\text{mms}^{-1}$ )	G (%)
NASICON 2	Db1	0.38	0.37	0.39	28
	Db2	0.29	0.81	0.65	72
NASICON 1	Db1	0.38	0.35	0.35	28
	Db2	0.30	0.90	0.62	72



**Figure 3:** A Mössbauer absorption spectrum of (a) NASICON 1 and (b) NASICON 2.

The appearance of vitreous phase is confirmed via examination of the texture of the materials via scanning electron microscopy (SEM) in various magnifications, giving a clear idea about the homogeneous distribution of the crystalline  $\text{Na}_3\text{Fe}_2(\text{PO}_4)_3$  in the matrix of the vitreous phase (Figures 4 and 5). Figure 4 shows NASICON 1 before 600 °C treatment and after the treatment. The texture of the material is shown in different magnifications, specified on the images /10  $\mu$ , 1 $\mu$ , 0,5  $\mu$ , respectively/. It can clearly be seen that after thermal treatment the material loses its grainy texture and acquires a homogeneous vitreous appearance. The same process is observed for NASICON 2, shown in Figure 5. It is observed, however, that the homogeneous vitreous appearance of NASICON 2, synthesized in the absence of colloid  $\text{SiO}_2$  is not so strongly pronounced in comparison to NASICON 1 and total loss of grainy structure is not observed. It can be supposed that the colloid silicon dioxide in the form of a dispersion phase assists the homogeneous distribution via inhibition of the active phase aggregation in NASICON 1.

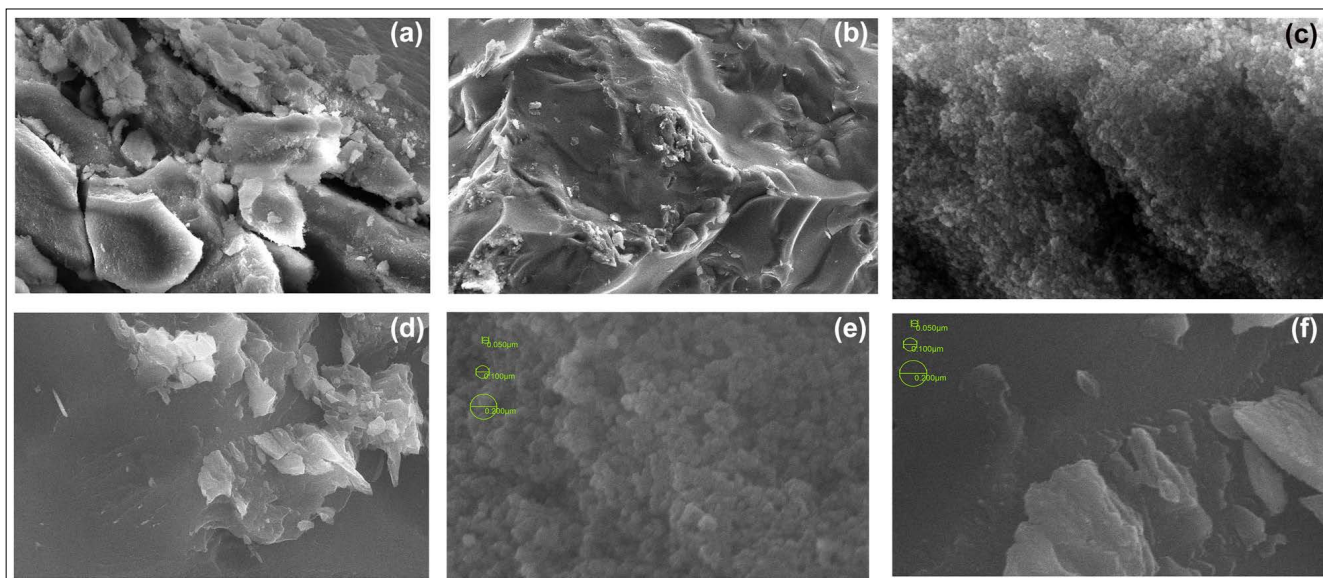


**Figure 4:** NASICON 1 thermal effects: (a), (c), (e) – before heat treatment, (b), (d), (f) – after firing at 600 °C.

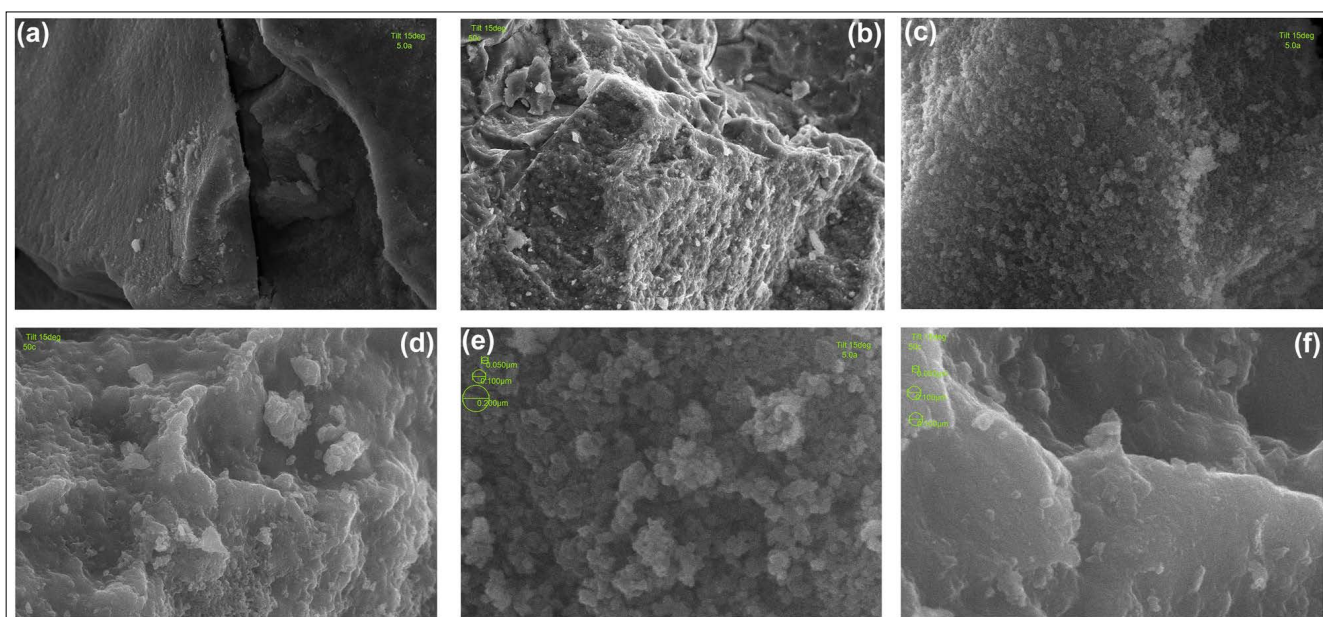


**Figure 5:** Occurrence of vitreous phase in NASICON 2 after thermal effects: (a), (c), (e) – before heat treatment, (b), (d), (f) – result at 600 °C.

The influence of the  $\text{SiO}_2$  is very clearly expressed also on the electrochemical properties of the materials. Figure 6 shows data from the examination of their activity under the following conditions: the object of testing is a coin cell type 2032. The results for a NASICON 1 half-cell first cycle capacity at C-rate 0.05 showed  $85 \text{ mAh g}^{-1}$  (expressed as mass for active material). Testing is conducted in a 1 M solution of  $\text{NaPF}_6$  in 1:1 (vol. %) EC-PC (ethylene carbonate – propylene carbonate), from 4.2 V to 1.5 V vs  $\text{Na}/\text{Na}^+$ . The assembly of the cell is done in a glove box (MBraun, Germany), where  $\text{O}_2$  and  $\text{H}_2\text{O}$  content are controlled below 0.1 ppm. Clearly expressed is the influence of the silicon dioxide on the system for  $\text{Na}_3\text{Fe}_2(\text{PO}_4)_3$  synthesis with electrochemical properties of NASICON 1. The test results for the electrochemical activity of the material without silicon dioxide (sample type NASICON 2) under the same conditions show greatly smaller capacity of  $1 \text{ mAh g}^{-1}$ , which confirms the promoting properties of the  $\text{SiO}_2$  matrix.

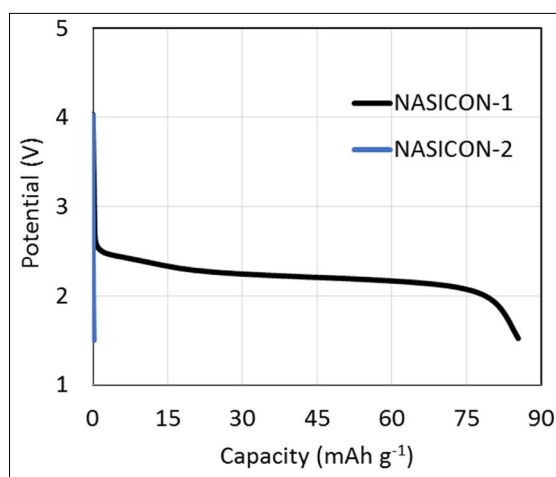


**Figure 6:** Electrochemical activity of two NASICON samples versus  $\text{Na}/\text{Na}^+$ , potential window 4.2–1.5 V (cell type 2032, electrolyte: 1 M  $\text{NaPF}_6$  in 1:1 (vol.%) EC-PC).

### Discussion

The present development shows a new route to synthesize NASICON-type material by using an "aqueous" method. The essence of the study is to prove the prospect of obtaining such a structure from a precursor  $\text{Na}_3\text{Fe}(\text{C}_2\text{O}_4)_3$ , using the characteristic properties of oxalates as complexing reagents. The questions it poses are important, such as: nature and structure of the glassy phase, chemical composition of this phase, conditions and chemical kinetics of formation. No less important is the "phase chemical composition - electrochemical activity" correlation of NASICON-type obtained in this way. The large difference in the electrochemical properties of NASICON 1 and NASICON 2 has its reason. Apart from the "composition-property" correlation, the reason must also be sought in the morphology, the dispersion characteristics of the particles and the formation of the crystallites at a temperature of around 600 °C. Taking into account the advantages of "wet" methods for the synthesis of substances, such as the possibility of precise technological control, automation and environmental friendliness, the synthesis of NASICON - type in this way is promising.

### Conclusion

A new method is described for  $\text{Na}_3\text{Fe}_2(\text{PO}_4)_3$  synthesis under controlled conditions in a water environment of iron oxalate precursor -  $\text{Na}_3\text{Fe}(\text{C}_2\text{O}_4)_3$ . The chemical transferring of ions in the oxalate environment between the iron and the phosphate precursor  $\text{NaH}_2(\text{PO}_4)$  is carried out in the presence of colloidal  $\text{SiO}_2$  (alkaline stabilized silicazol), creating a structure with high ion mobility of the sodium ions, thus imparting NASICON properties to the structure. These materials demonstrate promising electrochemical properties, but more research is needed. The results for a NASICON 1 half-cell first cycle capacity at C-rate 0.05 showed 85  $\text{mAh g}^{-1}$  in solution of 1 M  $\text{NaPF}_6$  in 1:1 (vol.%) EC-PC (ethylene carbonate – propylene carbonate), from 4.2 V to 1.5 V vs  $\text{Na}/\text{Na}^+$ .

### Research Funding

This work was partially supported by the EU through the European Regional Development Fund under project TK141 (2014–2020.4.01.15–0011).

### References

1. Kim T, Song W, Son DY, Ono LK, Qi Y (2019) Lithium-ion batteries: outlook on present, future, and hybridized technologies. *J Mater Chem A* 7: 2942-2964.
2. Wang T, Su D, Shanmukaraj D, Rojo T, Armand M, et al. (2018) Electrode Materials for Sodium-Ion Batteries: Considerations on Crystal Structures and Sodium Storage Mechanisms. *Electrochem Energ Rev* 1: 200-237.
3. Ramesh A, Tripathi A, Balaya P (2022) A mini review on cathode materials for sodium-ion batteries. *Int J Applied Ceramic Technology* 19: 913-923.
4. Gupta P, Pushpakanth S, Ali Haider M, Basu S (2022) Understanding the Design of Cathode Materials for Na-Ion Batteries. *ACS Omega* 7: 5605-5614.
5. Hagman LO, Kierkegaard P (1968) The Crystal Structure of  $\text{NaM}_2\text{IV}(\text{PO}_4)_3$ ;  $\text{MeIV} = \text{Ge}, \text{Ti}, \text{Zr}$ . *Acta Chem Scand* 22: 1822-1832.
6. Goodenough J, Hong HP, Kafalas J (1976) Fast  $\text{Na}^+$ -ion transport in skeleton structures. *Mater Res Bull* 11: 203-220.
7. Hong HYP (1976) Crystal structures and crystal chemistry in the system  $\text{Na}_{1+x}\text{Zr}_2\text{SixP}_3-x\text{O}_{12}$ . *Mater Res Bull* 11: 173-182.
8. Kale GM, Jafferson JM (2016) Solid-State Gas Sensors: Design and Fabrication. Reference Module in Materials Science and Materials Engineering 2001: 8731-8736.
9. Fanjat N, Soubeyrou JL (1992) Powder neutron diffraction study of  $\text{Fe}_2\text{Na}_3(\text{PO}_4)_3$  in the low temperature phase. *J Magn Magn Mater* 104: 933-934.
10. Anantharamulu N, Rao KK, Rambabu G, Kumar BV, Radha V, et al. (2011) A wide-ranging review on Nasicon type materials. *J Mater Sci* 46: 2821-2837.
11. Trad K, Carlier D, Croguennec L, Wattiaux A, Lajmi B, et al. (2010) A Layered Iron(III) Phosphate Phase,  $\text{Na}_3\text{Fe}_3(\text{PO}_4)_4$ : Synthesis, Structure, and Electrochemical Properties as Positive Electrode in Sodium Batteries. *J Phys Chem C* 114: 10034-10044.
12. Liu Y, Zhou Y, Zhang J, Xia Y, Chen T, et al. (2017) Monoclinic Phase  $\text{Na}_3\text{Fe}_2(\text{PO}_4)_3$ : Synthesis, Structure, and Electrochemical Performance as Cathode Material in Sodium-Ion Batteries. *ACS Sustain Chem Eng* 2: 1306-1314.
13. Lubomir Teoharov, Plamen Penev (2022) Method for obtaining sodium-iron phosphate  $\text{Na}_3\text{Fe}_2(\text{PO}_4)_3$  of NASICON type, Patent application BG/P/2022/113523.
14. Armentano D, De Munno G, Lloret F, Julve M (2005) Bis and tris(oxalato)ferrate(III) complexes as precursors of polynuclear compounds. *Cryst Eng Comm* 7: 57-63.
15. Alexandar Dragomirov, Lubomir Teoharov (2015) Method for processing refuse of flotation processing of ore concentrates containing iron. European Patent: EP 2998411 B1.
16. Lyubutin IS, Melnikov OK, Sigaryov SE, Terziev VG (1988) Phase transitions in  $\text{Na}_3\text{Fe}_2(\text{PO}_4)_3$ : An inside view. *Solid State Ionics* 31: 197-201.
17. Yu X, Day DE, Long GJ, Brow RK (1997) Properties and structure of sodium-iron phosphate glasses. *J Non-Crystal Solids* 215: 21-31.

**Copyright:** ©2023 Plamen Penev, et al. This is an open-access article distributed under the terms of the Creative Commons Attribution License, which permits unrestricted use, distribution, and reproduction in any medium, provided the original author and source are credited.